Saturation of turbulent helical dynamos

Guillaume Bermudez and Alexandros Alexakis*
Laboratoire de Physique de l'Ecole normale supérieure, ENS, Université PSL,
CNRS, Sorbonne Université, Université de Paris, F-75005 Paris, France
(Dated: May 2, 2022)

The presence of large scale magnetic fields in nature is often attributed to the inverse cascade of magnetic helicity driven by turbulent helical dynamos. In this work we show that in turbulent helical dynamos the inverse flux of magnetic helicity towards the large scales $\Pi_{\mathcal{H}}$ is bounded by $|\Pi_{\mathcal{H}}| \leq \epsilon k_\eta^{-1}$, where ϵ is the energy injection rate and k_η is the Kolmogorov magnetic dissipation wavenumber. Assuming the classical isotropic turbulence scaling for which $k_\eta \propto \ell_f^{-1} Rm^{3/4} \max[1, Pr]^{-1/4}$, with ℓ_f the forcing lengthscale, implies that the inverse flux of magnetic helicity decreases with Rm at least as $\Pi_{\mathcal{H}} \leq c\epsilon \ell_f Rm^{-3/4} \max[Pr, 1]^{1/4}$, where c is an order one constant. We demonstrate this scaling with Rm using direct numerical simulations of turbulent dynamos forced at intermediate scales. The results further indicate that nonlinear saturation is achieved by a balance between the inverse cascade and dissipation at domain size scales L and the saturation values of magnetic energy are bounded by $\mathcal{E}_{\mathrm{m}} \lesssim cL(\epsilon \ell_f)^{2/3} Rm^{1/4} \max[1, Pr]^{1/4}$. Numerical simulations also demonstrate this bound.

I. INTRODUCTION

Magnetic fields are observed in a plethora of astrophysical objects from planetary to galactic scales [1–3]. Their generation and sustainment is often attributed to dynamo action: their self-amplification by a continuous stretching and refolding of magnetic field lines due to the underlying (turbulent in most cases) flow [4]. In many cases the magnetic structures formed span the entire astrophysical object, reaching scales much larger than the small scale turbulence that generates them. The pioneering work of [5] showed that large scale magnetic fields can be generated from small scale flows if the advecting flow is helical. This result is based on an expansion for large scale separation and is referred as alpha-dynamo. However, such expansion can be formally done only below a critical value of Rm (the ratio of Ohmic to dynamic time scales). Above this critical value small scale dynamo action begins and the expansion ceases to be valid [6–8].

The validity of the alpha model is further questioned in the nonlinear regime for which the magnetic field feeds back to the velocity field through the Lorentz force. In [9, 10] it was argued that the growth of alpha dynamos saturates when the large scale magnetic field $\mathbf{B}$ becomes larger than $|\mathbf{B}| < U_{rms} Rm^{-1/2}$, where U_{rms} is the root mean square value of the velocity fluctuations. This gives a very weak magnetic field for most astrophysical applications for which $Rm \gg 1$.

An alternative way of explaining the formation of large magnetic fields is through the inverse cascade of helicity [11, 12]. This intrinsically non-linear mechanism (that is however compatible with alpha dynamos) predicts that magnetic helicity will be transferred by nonlinear interactions to larger scales. Indeed, several works that followed [13–16] demonstrated with numerical simulations

that when magnetic helicity is injected in a flow (by a dynamo or other mechanism), it cascades inversely to larger scales. These results however were performed on moderate values of Rm and the inverse cascade of magnetic helicity at large Rm is not tested. To our knowledge a quantitative understanding of how turbulent helical dynamos saturate with clear predictions of the saturating amplitude does not exist.

In this work we demonstrate by analytical arguments and numerical simulations that in dynamo flows, the inverse cascade of magnetic helicity is bounded from above by a decreasing power of Rm. Thus it cannot survive the infinite Rm limit. This leads to a prediction for the saturation amplitude of the magnetic field that we test with numerical simulations.

II. THEORETICAL ARGUMENTS

We begin by considering the MHD equations for the incompressible velocity $\mathbf{u}$ and magnetic field $\mathbf{b}$ given by

$$\partial_t \mathbf{u} + \mathbf{u} \cdot \nabla \mathbf{u} = -\nabla P + (\nabla \times \mathbf{b}) \times \mathbf{b} - \nu \nabla^2 \mathbf{u} + \mathbf{f}, \quad (1)$$
$$\partial_t \mathbf{b} = \nabla \times (\mathbf{u} \times \mathbf{b}) - \eta \nabla^2 \mathbf{b}, \quad (2)$$

in a cubic periodic domain of size $2\pi L$, with ν being the viscosity η the magnetic diffusivity and $\mathbf{f}$ an external mechanical force. The non-linear terms of this equation conserve the total energy $\mathcal{E} = \frac{1}{2}\langle |\mathbf{u}|^2 + |\mathbf{b}|^2 \rangle$ and magnetic helicity $\mathcal{H} = \frac{1}{2}\langle \mathbf{a} \cdot \mathbf{b} \rangle$, where the angular brackets stand for spatial average and $\mathbf{a} = -\nabla^{-2}\nabla \times \mathbf{b}$ is the vector potential. Their balance reads

$$\partial_t \mathcal{E} = \mathcal{I}_{\mathcal{E}} - \epsilon, \qquad \partial_t \mathcal{H} = -\epsilon_{\mathcal{H}}, \quad (3)$$

where $\mathcal{I}_{\mathcal{E}} = \langle \mathbf{f} \cdot \mathbf{u} \rangle$ is the energy injection rate, $\epsilon = \epsilon_u + \epsilon_b$ is the energy dissipation rate with $\epsilon_u = \nu \langle |\nabla \mathbf{u}|^2 \rangle$ the viscous dissipation rate and $\epsilon_b = \eta \langle |\nabla \mathbf{b}|^2 \rangle$ the Ohmic dissipation rate. Finally $\epsilon_{\mathcal{H}} = \eta \langle \mathbf{b} \cdot \nabla \times \mathbf{b} \rangle$ is the helicity generation/dissipation rate. The forcing $\mathbf{f}$ is assumed to

---
* alexakis@phys.ens.fr

act on a scale $\ell_f \ll L$ while dissipation acts at the smaller viscous scale ℓ_ν and Ohmic scale ℓ_η. For large Reynolds number $Re = \epsilon^{1/3}\ell_f^{4/3}/\nu$ and large magnetic Reynolds number $Rm = \epsilon^{1/3}\ell_f^{4/3}/\eta$, the dissipation length scales ℓ_ν, ℓ_η scale like [17]

$$\ell_\nu \propto \ell_f Re^{-3/4} \quad \text{and} \quad \ell_\eta \propto \ell_f Rm^{-3/4} \qquad (4)$$

for $Pm = \nu/\eta \le 1$ while for $Pr \ge 1$

$$\ell_\nu \propto \ell_f Re^{-3/4} \quad \text{and} \quad \ell_\eta \propto \ell_f Rm^{-3/4} Pm^{1/4}. \qquad (5)$$

At intermediate scales ℓ (so called inertial scales $\ell_f \ll \ell \ll \ell_\eta, \ell_\nu$), there is a constant flux of energy across scales given by

$$\Pi_{\mathcal{E}}(k) = \langle \mathbf{u}_k^< \cdot (\mathbf{u} \cdot \nabla \mathbf{u} - \mathbf{b} \cdot \nabla \mathbf{b}) - \mathbf{b}_k^< \cdot (\nabla \times \mathbf{u} \times \mathbf{b}) \rangle, \quad (6)$$

where $\mathbf{u}_k^<, \mathbf{b}_k^<$ stand for the filtered velocity and magnetic field respectively so that only Fourier modes with wavenumbers of norm smaller than $k \propto 1/\ell$ are kept [18]. Conservation of energy by the non-linear terms implies that the energy flux at the inertial scales is constant in k and equals the energy dissipation rate $\Pi_{\mathcal{E}}(k) = \epsilon$.

Similarly, there is a flux of magnetic helicity

$$\Pi_{\mathcal{H}}(k) = -\langle \mathbf{b}_\mathbf{k}^< \cdot (\mathbf{u} \times \mathbf{b}) \rangle \qquad (7)$$

that also has to be constant at scales that dissipation plays no role. However, unlike energy, the forcing does not inject magnetic helicity which can be only generated or destroyed by the Ohmic dissipation at rate $\epsilon_{\mathcal{H}}$. Nonetheless if the forcing is helical the flow can transport magnetic helicity from the small Ohmic scales to ever larger scale $L' > \ell_f$ up until the domain size reached $L' \simeq L$ where a helical condensate will form. Conservation of magnetic helicity by the non-linear terms implies again that the flux of helicity at scales $L' \gg \ell \gg \ell_\eta$ has to be constant in $k \propto 1/\ell$ with $\Pi_{\mathcal{H}}(k) = \epsilon_{\mathcal{H}}$.

The two cascades, energy and helicity, are not independent and the first limits the later [19]. To show that, we write the magnetic field in Fourier space $\tilde{\mathbf{b}}_\mathbf{k}$ using the helical basis $\tilde{\mathbf{b}}_\mathbf{k} = b_\mathbf{k}^+ \mathbf{h}_\mathbf{k}^+ + b_\mathbf{k}^- \mathbf{h}_\mathbf{k}^-$ where

$$\mathbf{h}^\pm = \frac{\mathbf{e} \times \mathbf{k} \times \mathbf{k}}{\sqrt{2}|\mathbf{e} \times \mathbf{k} \times \mathbf{k}|} \pm i \frac{\mathbf{e} \times \mathbf{k}}{\sqrt{2}|\mathbf{e} \times \mathbf{k}|} \qquad (8)$$

are the eigenvectors of the curl operator with $\mathbf{e}$ an arbitrary vector [20, 21]. By doing that we can write the magnetic energy spectrum as $E_b(k) = E_b^+(k) + E_b^-(k)$ and the magnetic helicity spectrum as $H(k) = (E_b^+(k) - E_b^-(k))/k$ where $E_b^\pm(k)\mathrm{d}k = \sum_{k \le |\mathbf{k}| < k+\mathrm{d}k} |b_\mathbf{k}^\pm|^2$ is the sum of the energy of the $b^\pm$ Fourier modes on a spherical shell of width $\mathrm{d}k$ and radius k. Since magnetic helicity is primarily generated at Ohmic wavenumbers $k_\eta = 1/\ell_\eta$

for any wavenumber k in the range $k \le k_\eta$ we can write

$$\begin{aligned}
|\Pi_{\mathcal{H}}(k)| &= |\epsilon_{\mathcal{H}}| \\
&\simeq \eta \left| \int_k^\infty q[E_b^+(q) - E_b^-(q)]\mathrm{d}q \right| \\
&\le \eta k^{-1} \int_k^\infty q^2 \left| E_b^+(q) + E_b^-(q) \right| \mathrm{d}q \\
&= k^{-1}\epsilon_b
\end{aligned} \qquad (9)$$

Choosing as k the largest allowed $k \simeq k_\eta$ and adding the viscous damping ϵ_u/k_η we obtain our final result

$$|\Pi_{\mathcal{H}}(k)| \le \epsilon/k_\eta. \qquad (10)$$

In other words the flux of magnetic helicity is bounded by the energy injection rate divided by the Ohmic dissipation wavenumber k_η. Note that this bound is saturated if the magnetic field at small scales is fully helical. If not, $|\Pi_{\mathcal{H}}|$ can be much smaller than (10). Using the estimates for k_η for isotropic MHD turbulence we obtain

$$|\Pi_{\mathcal{H}}(k)| \le c\epsilon k_f^{-1} Rm^{-3/4} \max[1, Pr]^{1/4}, \qquad (11)$$

where c is an order one constant. Given the very large values of Rm in nature this gives very little hope of observing such fluxes.

However, despite having a diminishing flux of magnetic helicity for large Rm, this does not mean that large scale dynamos cannot be observed. In a finite domain of size L a magnetic helicity condensate will form. Its magnetic field amplitude B will be determined by a balance of magnetic helicity flux with the magnetic helicity dissipation at that scale so that $\Pi_{\mathcal{H}} \propto \eta B^2/L$. Using the previous estimate for the flux leads to the prediction for the large scale energy $\mathcal{E}_m = B^2$ given by

$$\mathcal{E}_m \lesssim \epsilon^{2/3} L k_f^{1/3} Rm^{1/4} \max[1, Pr]^{1/4}. \qquad (12)$$

We note that a very long time $T \sim (B^2 L)/\Pi_{\mathcal{H}} \propto Rm$ would be required for such a field to be formed. Furthermore if there is an other η-independent mechanism for magnetic helicity saturation, like magnetic helicity expulsion [22, 23], then the amplitude of the large scale magnetic field will diminish to zero as $Rm \to \infty$.

Finally we note that this result is based on strong turbulence scaling of k_η. One can argue that as the large scale magnetic field builds up the relation between k_η and Rm can change from that of strong turbulence to that of weak turbulence [24] or turbulence driven by the large scale magnetic shear [25]. Both of these options lead to a faster increase of $\mathcal{E}_m$ with Rm as $\mathcal{E}_m \lesssim \epsilon^{2/3} L^{5/6} k_f^{-8/15} Rm^{2/5}$ that is not found however in the numerical studies that follow.

III. NUMERICAL SIMULATIONS

To demonstrate the above arguments we perform a series of numerical simulations that solve the MHD equations (1–2) using the pseudo-spectral code GHOST [26] in
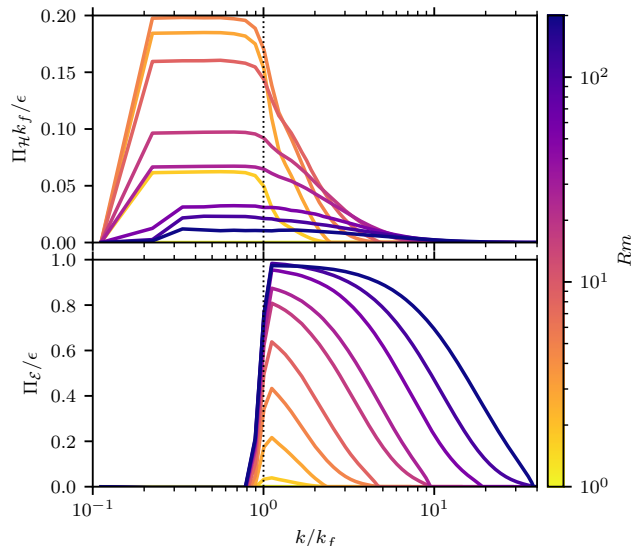
FIG. 1. Magnetic helicity flux $\Pi_{\mathcal{H}}$ (top) and total energy flux $\Pi_{\mathcal{E}}$ (bottom) for several values of the magnetic Reynolds number Rm for $k_f/k_0 = 8$.
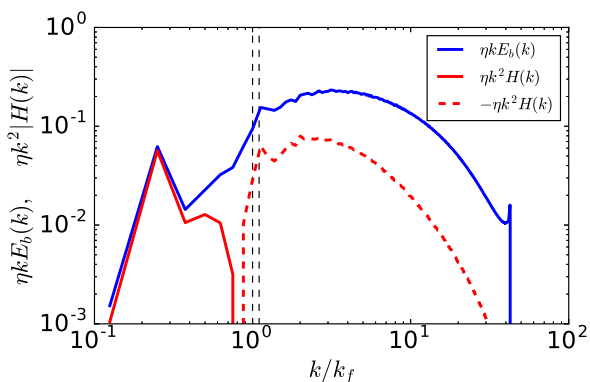

FIG. 2. Magnetic helicity dissipation/generation spectrum $\eta k^2 H(k)$ and normalized magnetic energy spectrum $\eta k E_b(k)$ for the case with hypo-dissipation with $k_f/k_0 = 8$ and the largest attained magnetic Reynolds number Rm.

a cubic domain of side $2\pi L$ with a fully helical random delta correlated forcing at wavenumber $k_f = 1/\ell_f$ that fixes the energy injection rate ϵ. The Prandtl number $Pm = \nu/\eta$ was set to unity for all runs. The resolution used varied from 128^3 grid points to 1024^3 grid points for the largest Rm. The resolution was chosen so that the largest inertial range is obtained while remaining well resolved with a clear dissipation wavenumber range.

As a first step to accommodate for the the large scale pile up of magnetic helicity we introduce a magnetic hypo-dissipation term $\eta_h \nabla^{-2} \mathbf{b}$ in (2) that arrests large scale magnetic helicity. With the inclusion of this term, the simulations reach quickly a steady state where the helicity generated at the small scales by $\epsilon_{\mathcal{H}}$ is transported and dissipated at the largest scales by hypo-dissipation.
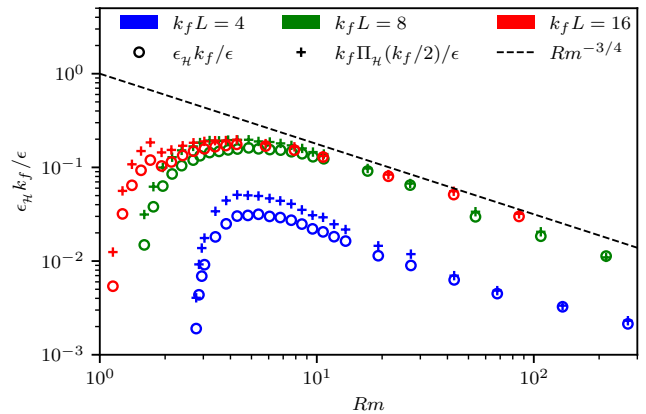
Figure 1 shows the magnetic helicity flux (top) and

FIG. 3. Magnetic helicity generation rate $\epsilon_{\mathcal{H}}$ (circles) and magnetic flux $\Pi_{\mathcal{H}}(k_f/2)$ (crosses) as a function of the magnetic Reynolds number Rm for three different values of $k_f L = 4$ (blue), $k_f L = 8$ (green) and $k_f L = 16$ (red).

energy flux (bottom) for a series of runs varying Rm as shown in the legend for $k_f L = 8$. The energy flux shows its classical behavior increasing as Rm is increased, approaching its maximal value $\Pi_{\mathcal{E}} \sim \epsilon$ in the inertial range. On the other hand, $\Pi_{\mathcal{H}}(k)$ first starts to increase with Rm once the dynamo onset is crossed, reaches a maximum and then starts to decrease again. The magnetic helicity generation spectrum $\eta k^2 H(k)$ for the largest Rm is shown in figure 2. Solid line corresponds to positive values of $\eta k^2 H(k)$ while dashed line corresponds to negative values of $\eta k^2 H(k)$, thus negative magnetic helicity is generated at the smallest scales. In the same plot we show the normalized magnetic energy spectrum $\eta k E_b(k)$ that bounds $\eta k^2 |H(k)| \leq \eta k E_b(k)$ with the equality corresponding to a fully helical magnetic field.

The dependence of the magnetic helicity cascade with Rm is best seen in figure 3 where the magnetic helicity generation rate $\epsilon_{\mathcal{H}} k_f/\epsilon$ (circles) and the magnetic helicity flux $\Pi_{\mathcal{H}}(k)$ at $k = k_f/2$ (crosses) are plotted as a function of Rm for three different scale separations $k_f L = 4, 8, 16$ in a log-log plot. All series show an initial increase of $\epsilon_{\mathcal{H}}$ and $\Pi_{\mathcal{H}}(k_f/2)$ followed afterwards by a power-law decrease with $\epsilon_{\mathcal{H}} \simeq \Pi_{\mathcal{H}}(k_f/2)$. The dashed lines give the predicted scaling $Rm^{-3/4}$ that appears to fit very well the observed power verifying our prediction in (11).

A second series of numerical simulations with $k_f L = 8$ were performed without the hypo-viscous term. The simulations were run for very long times until a steady state is reached such that magnetic energy does not increase further. The time scale to reach saturation is very long and this has limited us to use grids of size up to 512^3 and values of Rm four times smaller than the case with hypo-dissipation. Figure 4 shows with a red line the magnetic helicity dissipation spectrum $\eta k^2 H(k)$ for the largest Rm examined for these runs. Positive magnetic helicity is concentrated in a large scale condensate at $k = 1/L = k_f/8$ while it is negative for all smaller scales. As in figure 2 we also show $\eta k E_b(k)$ with a blue line.
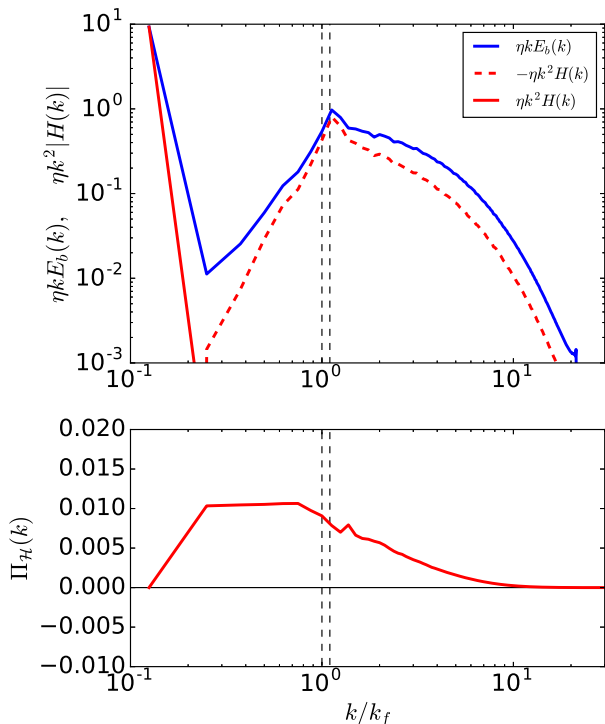
FIG. 4. Top panel: Magnetic helicity dissipation/generation spectrum $\eta k^2 H(k)$ and normalized magnetic energy spectrum $\eta k E_b(k)$ for the runs with no hypo-dissipation, with $k_f L = 8$ and the largest attained magnetic Reynolds number Rm. Bottom panel: magnetic helicity flux for the same run.

FIG. 5. Saturation of the magnetic energy $\mathcal{E}_{\mathrm{m,sat}}$ as a function of the magnetic Reynolds number Rm for $k_f L = 8$ in a log-log plot. The dashed line gives the prediction $Rm^{1/4}$. Inset: same figure in lin-log plot.

Note that while the large scales are fully helical small scales are less. The amplitude of the large scale condensate (at the smallest $k = k_f/8$) is so large that despite the small value of η the negative magnetic helicity generated at small scales by Ohmic diffusion is balanced by the positive helicity generated at the largest scale again by Ohmic diffusion. This leads to the flux of (negative) helicity from small to large scales shown in the lower panel of the same figure.

The balance between the magnetic helicity generated at small scales and dissipated at the large leads to the prediction (12) of a weak power-law increase of magnetic energy $\mathcal{E}_m$ with Rm. Figure 5 shows $\mathcal{E}_m$ as a function of Rm in a log-log plot. The last three points appear to agree with the predicted power-law. The range of values of Rm compatible with this law is however rather limited and smaller power-laws or logarithmic increase cannot be excluded. In the inset of the same figure we show the same data in a lin-log plot demonstrating that the data could also be fitted to a logarithmic increase. A logarithmic increase, if true, is still compatible with the bound (12) but does not saturate it, and would imply that small scales become less and less helical as Rm is increased.
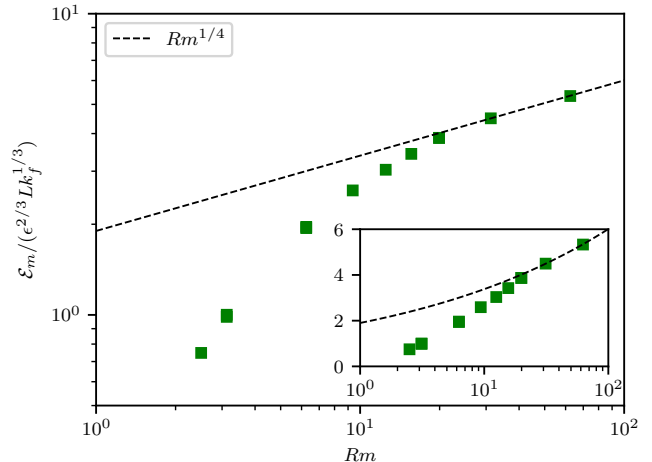
IV. CONCLUSION

The present work gives for the first time estimates for the flux of magnetic helicity and the saturation of the magnetic field for the nonlinear state of a large Rm turbulent helical dynamo. Remarkably, even for asymptotically large values of Rm it has been shown that the magnetic helicity flux still depends on Rm and in fact it has to decrease at least as fast as $\Pi_{\mathcal{H}} \leq \epsilon/k_\eta \sim \epsilon/k_f Rm^{-3/4}$. This analytical result has also been clearly demonstrated by numerical simulations that are shown to follow this upper bound scaling. This excludes any inviscid nonlinear theory for large scale dynamos from being realized!

Furthermore it was shown that saturation is achieved by a balance of the inverse magnetic helicity flux with the helicity dissipation at the condensate scale. This has lead to the prediction that the magnetic field amplitude at steady state is smaller than $Rm^{1/4}$. Numerical simulations are compatible with this result although the covered range of Rm cannot exclude other small power-laws or logarithmic increase with Rm.

It is important to note that these results are based on magnetic helicity conservation and are independent of the actual dynamo mechanism involved (alpha or other). They are thus rather general. Finally, we stress that if an η−independent mechanism exists at large scales to saturate the large scale magnetic helicity (like magnetic flux expulsion), our result (10) implies that no dominant large scale magnetic field will be present in the $Rm \to \infty$ limit.

The present results have critical implications for large magnetic fields in astrophysical systems and their origin.

[1] E. Falgarone and T. Passot, *Turbulence and magnetic fields in astrophysics*, Vol. 614 (Springer, 2008).

[2] A. Ruzmaikin, D. Sokoloff, and A. Shukurov, *Magnetic Fields of Galaxies*, Astrophysics and Space Science Library (Springer Netherlands, 1988).

[3] E. N. Parker, *Cosmical magnetic fields: Their origin and their activity* (Oxford university press, 1979).

[4] H. K. Moffatt, *Field generation in electrically conducting fluids*, Vol. 2 (1978).

[5] M. Steenbeck, F. Krause, and K.-H. Rädler, Berechnung der mittleren lorentz-feldstärke für ein elektrisch leitendes medium in turbulenter, durch coriolis-kräfte beeinflußter bewegung, Zeitschrift für Naturforschung A **21**, 369 (1966).

[6] S. Boldyrev, F. Cattaneo, and R. Rosner, Magnetic-field generation in helical turbulence, Physical review letters **95**, 255001 (2005).

[7] F. Cattaneo and D. Hughes, Problems with kinematic mean field electrodynamics at high magnetic reynolds numbers, Monthly Notices of the Royal Astronomical Society: Letters **395**, L48 (2009).

[8] A. Cameron and A. Alexakis, Fate of alpha dynamos at large r m, Physical review letters **117**, 205101 (2016).

[9] S. I. Vainshtein and F. Cattaneo, Nonlinear restrictions on dynamo action, The Astrophysical Journal **393**, 165 (1992).

[10] D. Hughes, The mean electromotive force at high magnetic reynolds numbers, Plasma Physics and Controlled Fusion **50**, 124021 (2008).

[11] U. Frisch, A. Pouquet, J. Léorat, and A. Mazure, Possibility of an inverse cascade of magnetic helicity in magnetohydrodynamic turbulence, Journal of Fluid Mechanics **68**, 769 (1975).

[12] A. Pouquet, U. Frisch, and J. Léorat, Strong mhd helical turbulence and the nonlinear dynamo effect, Journal of Fluid Mechanics **77**, 321 (1976).

[13] A. Pouquet and G. Patterson, Numerical simulation of helical magnetohydrodynamic turbulence, Journal of Fluid Mechanics **85**, 305 (1978).

[14] A. Brandenburg, The inverse cascade and nonlinear alpha-effect in simulations of isotropic helical hydromagnetic turbulence, The Astrophysical Journal **550**, 824 (2001).

[15] A. Alexakis, P. D. Mininni, and A. Pouquet, On the inverse cascade of magnetic helicity, The Astrophysical Journal **640**, 335 (2006).

[16] W.-C. Müller, S. K. Malapaka, and A. Busse, Inverse cascade of magnetic helicity in magnetohydrodynamic turbulence, Physical Review E **85**, 015302 (2012).

[17] A. A. Schekochihin, S. A. Boldyrev, and R. M. Kulsrud, Spectra and growth rates of fluctuating magnetic fields in the kinematic dynamo theory with large magnetic prandtl numbers, The Astrophysical Journal **567**, 828 (2002).

[18] D. Biskamp, *Magnetohydrodynamic turbulence* (Cambridge University Press, 2003).

[19] A. Alexakis and L. Biferale, Cascades and transitions in turbulent flows, Physics Reports **767**, 1 (2018).

[20] F. Waleffe, The nature of triad interactions in homogeneous turbulence, Physics of Fluids A: Fluid Dynamics **4**, 350 (1992).

[21] M. Linkmann, A. Berera, M. McKay, and J. Jäger, Helical mode interactions and spectral transfer processes in magnetohydrodynamic turbulence, Journal of Fluid Mechanics **791**, 61 (2016).

[22] F. Rincon, Helical turbulent nonlinear dynamo at large magnetic reynolds numbers, Physical Review Fluids **6**, L121701 (2021).

[23] F. Cattaneo, G. Bodo, and S. Tobias, On magnetic helicity generation and transport in a nonlinear dynamo driven by a helical flow, Journal of Plasma Physics **86** (2020).

[24] S. Galtier, S. Nazarenko, A. C. Newell, and A. Pouquet, A weak turbulence theory for incompressible magnetohydrodynamics, Journal of plasma physics **63**, 447 (2000).

[25] A. Alexakis, Large-scale magnetic fields in magnetohydrodynamic turbulence, Physical Review Letters **110**, 084502 (2013).

[26] P. D. Mininni, D. Rosenberg, R. Reddy, and A. Pouquet, A hybrid mpi–openmp scheme for scalable parallel pseudospectral computations for fluid turbulence, Parallel computing **37**, 316 (2011).